SAND2020-8198J

Dissolvable Template Nanoimprint Lithography: A Facile and Versatile Nanoscale Replication Technique

Junho Oh[1†], Jacob B. Hoffman[2], Sungmin Hong[2], Kyoo Dong Jo[2], Jessica Román-Kustas[2,3], Julian H. Reed[2], Catherine E. Dana[4], Donald M. Cropek[2], Marianne Alleyne[4,5*], Nenad Miljkovic[1,6,7,8*]*

[1]Department of Mechanical Science and Engineering, University of Illinois at Urbana–Champaign, Urbana, IL 61801, USA

[2]Construction Engineering Research Laboratory, U.S. Army Engineer Research and Development Center, Champaign, IL 61822, USA

[3]Materials Reliability, Sandia National Laboratories, Albuquerque, NM, 87123, USA

[4]Department of Entomology, University of Illinois at Urbana–Champaign, Urbana, IL 61801, USA

[5]Beckman Institute of Advanced Science and Technology, University of Illinois at Urbana–Champaign, Urbana, IL 61801, USA

[6]Department of Electrical and Computer Engineering, University of Illinois at Urbana–Champaign, Urbana, IL 61801, USA

[7]Materials Research Laboratory, University of Illinois at Urbana–Champaign, Urbana, IL 61801, USA

[8]International Institute for Carbon Neutral Energy Research (WPI-I2CNER), Kyushu University, 744 Moto-oka, Nishi-ku, Fukuoka, 819-0395, Japan

[†] The author is currently at University College London, London, WC1E 7JE, United Kingdom.
*Authors to whom correspondence should be addressed. Electronic mail: Nenad Miljkovic: nmiljkov@illinois.edu; Marianne Alleyne: vanlaarh@illinois.edu; Donald Cropek: Donald.M.Cropek@usace.army.mil.

Abstract

Nanoimprinting lithography (NIL) is a next-generation nanofabrication method, capable of replicating nanostructures from original master surfaces. Here, we develop highly scalable, simple, and non-destructive NIL using a dissolvable template. Termed dissolvable template nanoimprinting lithography (DT-NIL), our method utilizes an economic thermoplastic resin (commercial nail polish) to fabricate nanoimprinting templates, which can be easily dissolved in simple organic solvents. We used the DT-NIL method to replicate cicada wings (*Neotibicen pruinosus*) which have surface nanofeatures of ~100 nm in height. The master, template and replica surfaces showed a $\gtrsim$94% similarity based on the measured diameter and height of the nanofeatures. The versatility of DT-NIL was also demonstrated with the replication of re-entrant, multi-scale, and hierarchical features on fly wings (*Sarcophaga bullata*), as well as hard silicon wafer based artificial nanostructures. The DT-NIL method can be performed under ambient conditions with the use of inexpensive and commercially available materials and equipment. Our work opens the door to opportunities for economical and high-throughput nanofabrication processes for replicating nanofeatures of various surfaces.

Keywords

Nanoimprinting, template, insect wing, nanostructures, nanomanufacturing

Nanoimprinting lithography (NIL) is one of the most promising next-generation methods for fabricating nanoscale patterns and features on surfaces. Instead of using methods involving photomasks or techniques that directly scribe or etch features onto the surface of interest, NIL uses an original sample (herein called a master) to first fabricate a mold (herein called a template). Replicas are produced from a template having the negative image of the original master, with all of the nano- or microscale structures present on the master. A template can produce thousands of replicates, which allows for high duplicability and throughput.[1, 2]

First reported in the 1990s[1], research on NIL has progressed to enable high-resolution replication, down to ~10 nm scales with high throughput. The earliest nanoimprinting method, now called thermal NIL, requires elevated temperatures (~200°C) and high pressures (~40 bar) during the molding process to produce templates from a master surface.[2-4] These high temperature and pressure conditions impose limitations on the selection of the original sample for reproduction. Newer methods have enabled the reduction of harsh conditions by developing room temperature nanoimprint lithography (RT-NIL),[4-6] UV-curable NIL (UV-NIL),[7-9] and direct NIL[10-12] to achieve larger fabrication areas,[13, 14] rapid fabrication,[15, 16] and easier release of the template.[17, 18] However, even state-of-the-art NIL techniques remain limited due to high fabrication temperature, pressure, or manufacturing costs.[2, 19]

In this study, we develop scalable, simple, and cost-effective dissolvable template nanoimprinting lithography (DT-NIL). We demonstrate DT-NIL for template and replica fabrication using both natural (insect wing masters) and engineered (silicon masters) surfaces possessing nanoscale features. The DT-NIL method fabricates a dissolvable template from a master and enables the scalable production of replicas from the dissolvable template. The method employs simple methods at room temperature and atmospheric pressure and uses materials

accessible outside of laboratory cleanrooms, such as nail polish and rubbing alcohol. In addition, nail polish is non-toxic and biocompatible, thus eliminating the need for the use of toxic chemicals used in other NIL applications. We demonstrate the nanoscale resolution of DT-NIL by replicating nanofeatures present on various master surfaces onto both hard and soft materials.

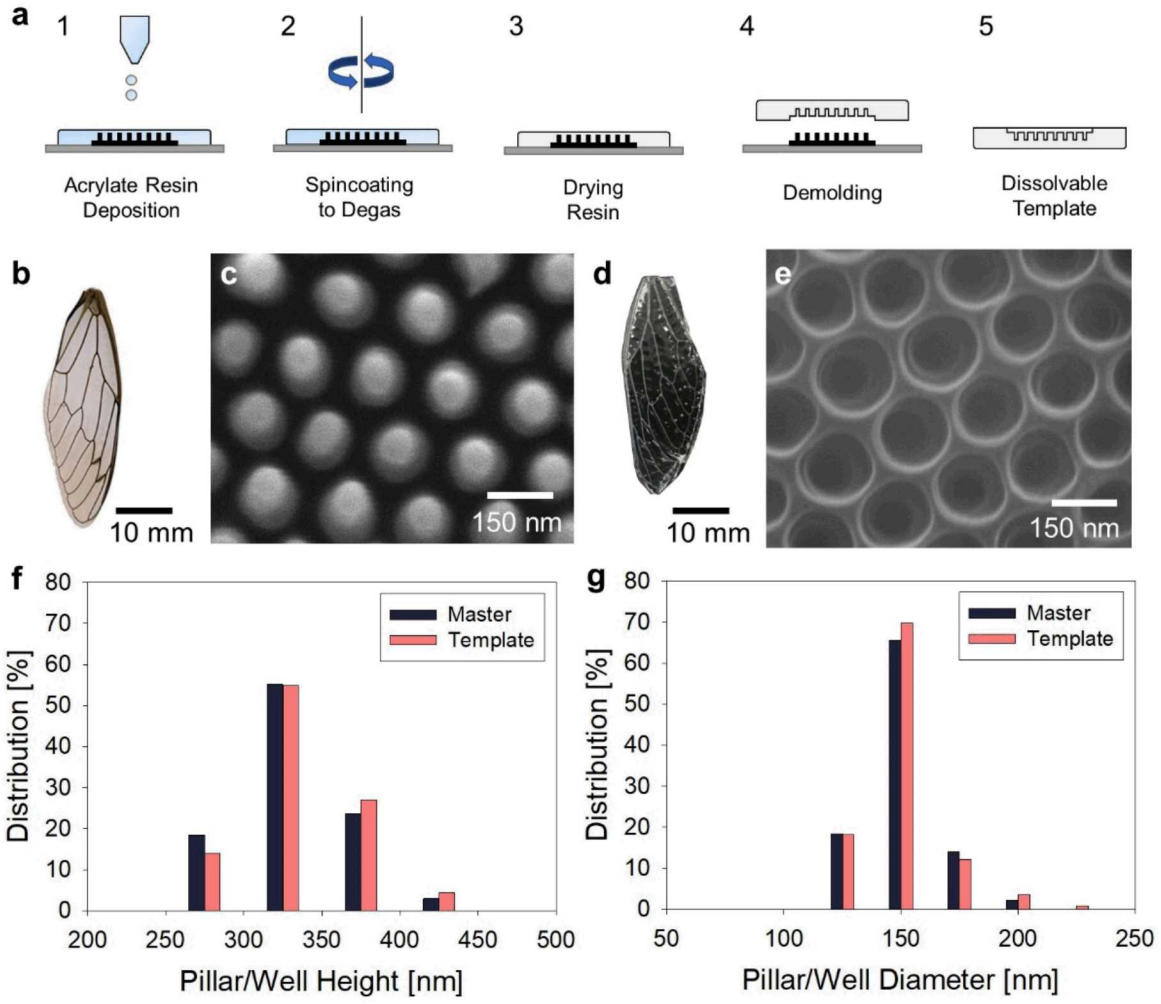

re

Figure 1. (a) Fabrication process schematics for DT-NIL showing 1) deposition of 0.1 mL/cm^2 of acrylic resin on the template surface, 2) spin coating acrylic resin at 500 rpm for 60 seconds (optional, see Supporting Information S.2), 3) drying acrylic resin at room temperature, 4) demolding template from the master surface, 5) resulting in a dissolvable acrylic resin template. (b) Photograph of an original (master) *Neotibicen pruinosus* cicada wing with (c) corresponding scanning electron micrograph (SEM) of the nanopillar features on the original wing having mean pillar heights (h_{avg}) = 332 ± 28 nm and mean diameters (d_{avg}) = 148 ± 8 nm, as measured using atomic force microscopy (AFM).[20] (d) Photograph of the dissolvable template imprinted from the original wing master shown in (b) with corresponding (e) SEM showing h_{avg} = 337 ± 32 nm and d_{avg} = 146 ± 8 nm as measured with AFM. (f) Height and (g) diameter distributions of nanopillars on the original wings and nanowells created on the template obtained with AFM.

For the template material, we used a readily available quick-drying nail polish (Sally Hansen, InstaDri top coat nail polish), consisting of a mixture of solvents, several film forming agents, plasticizers, and other commercial additives. Figure 1a illustrates the DT-NIL template fabrication process. Prior to template fabrication, the master surface was cleaned through sequential sonication in acetone, ethanol, and deionized (DI) water, followed by drying in a clean nitrogen (N_2) stream. Flexible master samples, such as insect wings, were adhered to a glass microscope slide using double-sided mounting tape. After mounting, ~2 mL/cm^2 of nail polish was deposited on the master and spread *via* spin coating for 60 seconds at 500 rpm. The template thickness after spin coating at 500 rpm was approximately 3-5 μm. After spin coating, the nail polish was left to cure at room temperature for 30 minutes. Note, spin coating is optional for the nail polish used as the fabricated template showed similar feature heights to the template fabricated by drop casting without spin coating (Supporting Information S.2). However, if a dissolvable resin with a higher viscosity is used, spincoating will be necessary. The resulting template thickness by drop casting was ~10 μm. Undercured tacky nail polish could result in template stretching or tearing during the demolding process. Meanwhile over-cured nail polish (> 6 hours) becomes too brittle to be removed in a single piece. During drying and curing, the nail polish resin does not completely evaporate, maintaining its initial contact line. In addition, the nail polish does not contain colloidal particles, eliminating the coffee ring effect[21, 22]. After curing, the nail polish was carefully peeled off from the master and left to cure further between two sterile microscope glass slides to prevent warping due to the residual stresses from peeling.[23] Although the force required for peeling the template from the master varies with structure length scale and chemistry, the force is minimal and easily accomplished manually by using forceps to hold the template without damaging either the master or the template. After cleaning, the master

surface could be used to generate additional templates, demonstrating reproducibility (For additional notes on reproducibility and the template generation process, see Supporting Information S.3).

We used cicada wings (*Neotibicen pruinosus*) as the master surface for template fabrication. (For cicada collection and master sample preparation, see Supporting Information S.4.) This cicada species was chosen due to the nanopillar features that exist on the wing surface,[20] making it an interesting biological surface for demonstrating the versatility and resolution of DT-NIL. Figure 1(b) shows a representative image of a cicada wing along with a top-view scanning electron microscopy (SEM) image (Fig. 1c) of the nanopillars. The nanopillars have a larger diameter at the base near the substrate, and a smaller diameter at the tip, consistent with findings from previous studies.[20, 24] Figure 1f and 1g show statistical data of nanofeatures on the wing surface derived from atomic force microscopy (AFM). The AFM results show that the master wing sample (black bars) had nanopillars with mean height (Fig. 1f) and width (Fig. 1g) of 332 ± 28 nm and 148 ± 7 nm, respectively (hereby in the text, the values are the mean ± standard deviation). A representative image of the nail polish template and the SEM micrograph of the negative features imprinted onto the template are shown in Figures 1d and e, respectively. The nanowell tapered from wide at the surface to narrow at the bottom, opposite from the original nanopillars on the wing master. AFM characterization of the imprinted nanowells (Figure 1f and 1g, red bars) shows that the mean well depth and diameter of the template was 337 ± 32 nm and 145 ± 8 nm, respectively. The distributions and mean heights and diameters of the nanopillars on the original cicada wings and the distributions and mean heights of the nanowells on the template showed excellent agreement, proving complete imprinting of the nanofeatures using DT-NIL.

As evident from the data obtained from AFM imaging shown in Fig. 1f and 1g, the dissolvable templates made from nail polish offer great flexibility and high fidelity at small scales down to ~20 nm (crevices between pillars) up to 100 nm (nanopillars) at room temperature and atmospheric pressure. The high resolution achieved using DT-NIL can be attributed to the properties of the nail polish. The surface energy of other commercially available nail polishes vary with formulations and additives, but are generally reported in the range of 30 - 40 mJ/m^2, with a viscosity between 0.1 - 0.5 Pa·s.[25, 26] Lower viscosity and surface energy resins, such as nail polish, are preferred for molding features completely without air inclusions and are therefore a logical template material for DT-NIL.

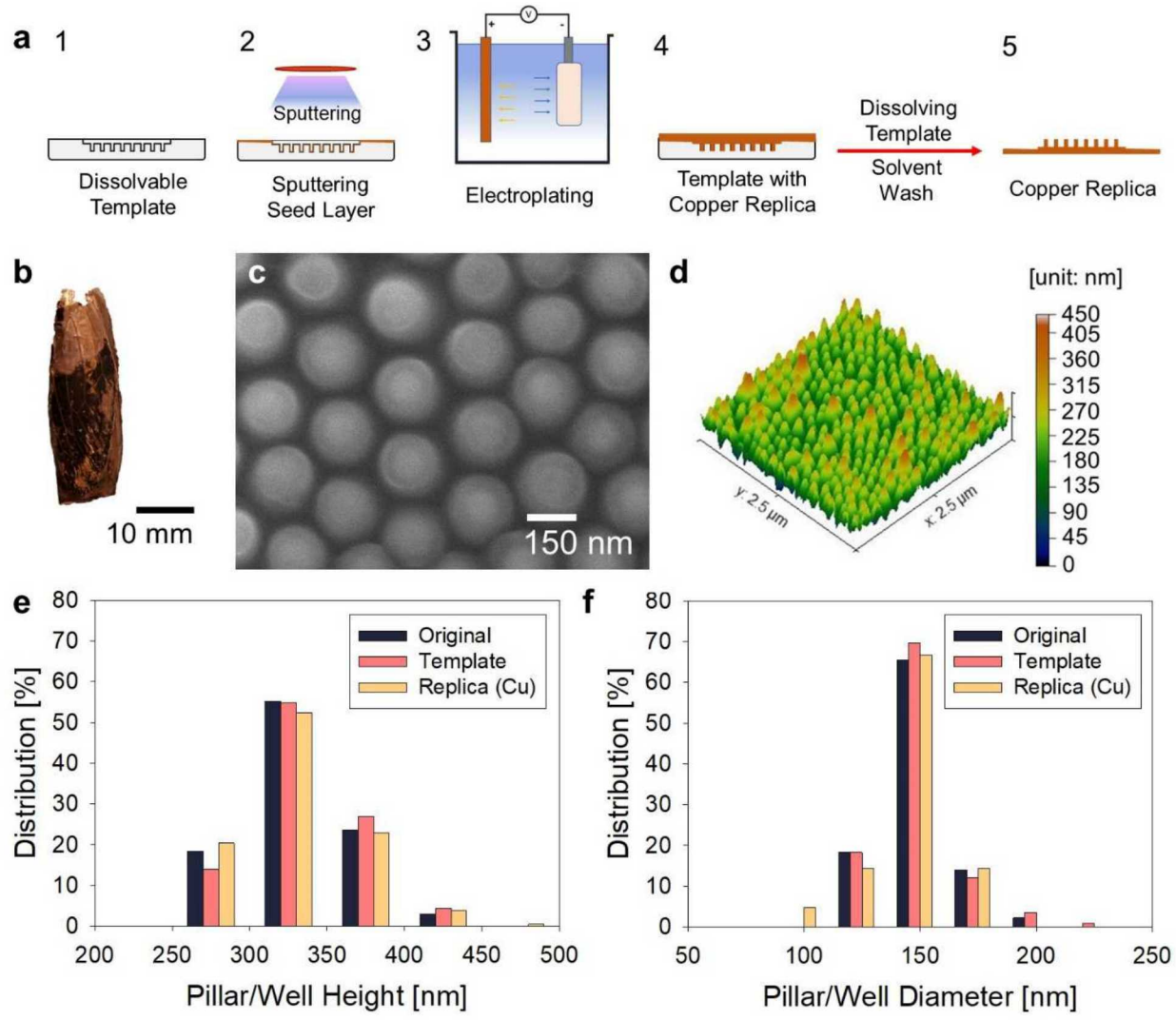

Figure 2. (a) Replication step schematics of the *Neotibicen pruinosus* cicada wing master fabricated using DT-NIL and metal electroplating. After 1) formation of the dissolvable template the fabrication steps include: 2) deposition of a conductive seed layer of copper (Cu, ~30-50 nm thick), 3) metal electroplating in an electroplating solution containing Cu ions (Cu^{2+}) for 30 minutes to deposit a dense layer of Cu on the seed layer and template, 4) solvent wash to dissolve the template using acetonitrile, isopropyl alcohol and DI water with agitation and gentle spraying, followed by drying in a clean N_2 stream, (b) Top-view photograph of the entire Cu wing replica with (c) corresponding SEM micrograph and (d) AFM images of the tip surface. (e) Height and (f) diameter distributions of nanopillars on the original master wings, nanowells, and Cu replicas on the dissolvable template obtained using AFM. The distribution shows that the Cu replica pillars had a height of 329 ± 32 nm and a diameter of 145 ± 8 nm.

After confirming that our template successfully imprinted nanostructures with high fidelity, we utilized the dissolvable template to make replicas of the cicada wings using two different materials and deposition techniques (Fig. 2a). First, we used electroplating of copper (Cu) to make a metallic cicada wing. Initially, a 50 nm seed layer of gold or Cu was sputtered onto the template to make it conductive. The resulting metal-coated template was determined to be superhydrophilic, with apparent advancing and apparent receding contact angles of $\theta_a^{app} = 12.4 \pm 3.7°$ and $\theta_r^{app} = 0°$, ensuring that the Cu plating solution would completely wet the nanowells during the plating process. To deposit Cu on the template, we used a commercially available Cu plating solution (Elevate Cu 6320, Technik Inc., USA). The pH of the plating solution was approximately 3 to 4 as measured using pH test paper. We maintained a relatively low current density (< 0.02 A/cm^2) to prevent the template from being burned by Joule heating. The low current density resulted in a slow deposition rate (0.74 μm/min) when depositing a ≈20 μm thick copper layer at 25°C (for deposition parameters, see Supporting Information S.5). Even though the 2-electrode electrodeposition method enabled us to replicate the master successfully, 3-point electrode electrodeposition might be preffered for other applications since it reduces current density to prevent Joule heating while operating at a constant voltage.

After Cu plating, the nail polish was dissolved by placing the template-replicate layers in an acetonitrile sonication bath for 3 minutes, followed by acetonitrile, ethanol and DI water washes using spray bottles. Spray washes, rather than further sonication, were used in the final steps of replica fabrication since spaying minimizes potential redeposition of dissolved template residue present in sonication baths. Figure 2b provides the visual evidence of wing nanostructure replication showing the differences between the area where nanopillars were replicated (dark brown) or not (bright coppery color). The area without proper nanopillar replication occurred for

two reasons. First, the template melted due to excessive joule heating where an alligator clip has direct contact. The copper could then be deposited on a partially detached Au seed layer or in cracks between the seed layer and the template. Note, even very minor cracks in templates can cause imperfection in the replication as Cu randomly deposited on the nanofeatures, usually concentrated in the peripheral area as seen in Fig. 2b. The distinct color difference likely arises from the passive antireflectivity.[27] Without reflection, the copper metal can absorb light across the visible spectrum, leading to the darker color observed similar to that seen from nanostructured copper oxide surfaces.[28] This is confirmed in SEM micrographs and AFM scans of the darker area, showing highly ordered and conformal nanopillar arrays over the surface (Fig. 2c,d).

The nanopillars present on the replicate had similar dimensions to those of the original master cicada wing, featuring a mean height and diameter of 329 ± 32 nm and 145 ± 8 nm, respectively (Figure 2e and f, yellow bars). This is a 99% replication of the original nanostructure mean height and a 98% replication of the mean diameter. Furthermore, replica, template, and master showed nanopillars/nanowells having similar height and diameter distributions extracted from AFM scans. Together, these two factors indicate high-resolution fabrication of Cu nanopillars.

To reproduce the superhydrophobic functionality of the original wing master, we coated the surface with heptadecafluorodecyltrimethoxysilane (HTMS, CAS #83048-65-1, Gelest Inc, USA). The functionalization resulted in an increase of apparent advancing and receding contact angles with water to θ_a^{app} = 158 ± 5 and θ_r^{app} = 153 ± 8° from θ_a^{app} <10° and θ_r^{app}<10°, indicating superhydrophobicity and showing our DT-NIL method can replicate functionality as well as structure. (For contact angle measurement details, see Supporting Information S.6).

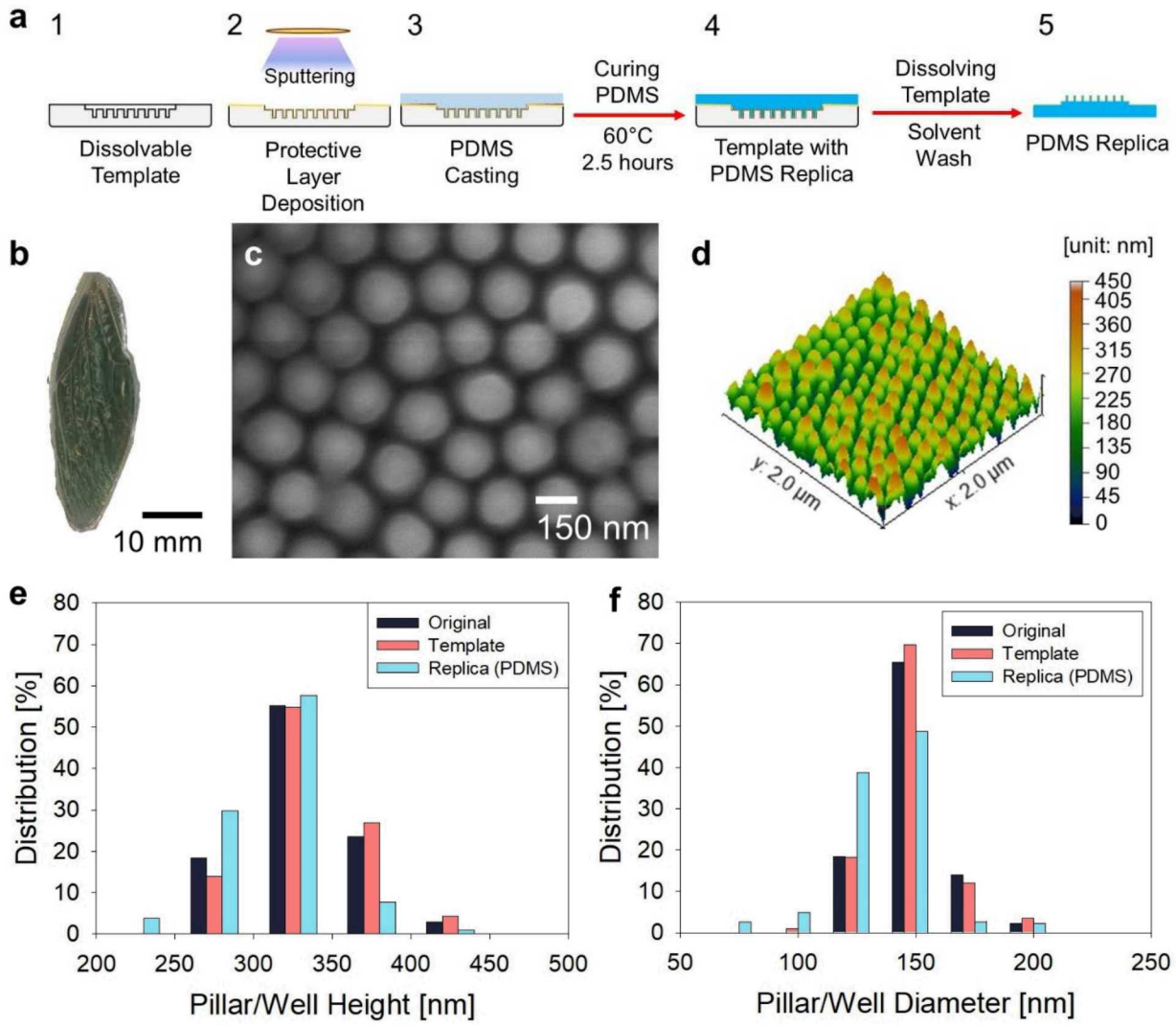

Figure 3. Fabrication of *Neotibicen pruinosus* cicada wing replicas using DT-NIL and polydimethylsiloxane (PDMS). (a) Detailed fabrication step schematics of the replica made from PDMS after 1) formation of the dissolvable template, the fabrication steps include: 2) deposition of an assistive Au layer (5 nm) to avoid structural collapse of the PDMS post-fabrication, 3) deposition and degassing of the PDMS, 4) PDMS curing for 2.5 hours at 60°C, 5) solvent wash to dissolve the template using acetonitrile, isopropyl alcohol and DI water with agitation and gentle spraying, followed by drying in an N_2 stream. (b) Image of the entire PDMS replica wing with corresponding (c) SEM and (d) AFM images. (e) Height and (f) diameter distributions of nanopillars on the original wings, nanowells on the dissolvable template, and PDMS replicas obtained using AFM. The distribution shows that the PDMS replica mean was 94.4% of the height and 106% of the diameter of the original wing master.

To further demonstrate the versatility of DT-NIL, we selected polydimethylsiloxane (PDMS) as a second material which is softer and more flexible than Cu. Figure 3a shows the general replica procedure using PDMS. First, a 5 nm gold layer was sputtered on the template surface to protect the replica from structural collapse. Next, we cast PDMS (Dow SYLGARD™ 184, Dow Corning, USA) onto the template using a typical soft lithography process.[29] In order to attain sufficient wetting to fill the template nanowells, PDMS (viscosity: 3.5 Pa·s) was diluted with hexamethyldisiloxane (HMDS, ClearCo, viscosity: 4.9×10^{-10} Pa·s) in a 1:0.1:0.5 PDMS base to PDMS initiator to HMDS ratio. The mixture was poured over the template and degassed under vacuum for 30 minutes. After degassing, the PDMS mixture was kept at 60□ for 2.5 hours to cure and to evaporate any residual HMDS. Normal PDMS curing temperatures (80□) resulted in replica surface wrinkling, due to the difference in thermal expansion coefficients between gold and PDMS. To prevent distortion due to thermal stress, the replica was left in the oven until it cooled down from 60□ to room temperature. The nail polish template was dissolved by placing the sample in a gentle bath of acetonitrile for 10 minutes with a solvent flow over the template, maintained using a Pasteur pipette. After most of the nail polish was dissolved, the sample was gently sonicated for 5 min in an acetonitrile bath and an isopropyl alcohol (IPA) bath, in sequence, to completely remove resin residue. Figure 3b shows a picture of the PDMS replica, and corresponding images of the PDMS nanopillar array using (c) SEM and (d) AFM. The gold coating sputtered onto the template was transferred to the replica, causing the entire surface to appear dull and dark. The color suggested that nanofeatures were present across the entire replica surface. The color arose due to the anti-reflectivity of the cicada wings caused by the periodic nanopillars,[30, 31] similar to the Cu replica. The presence of the nanopillar array was confirmed with both SEM and AFM, with mean height and diameter of 313 ± 31 nm and 136 ± 6 nm,

respectively (Figure 3e, f, cyan bars). The mean height and width measured on the PDMS replica were within ±6% of the dimensions of these features on the original master cicada wing and are within the within the uncertainty of the measurement and the limits of image processing, demonstrating the capability of DT-NIL to replicate features in PDMS with high resolution. The PDMS replicas showed a larger distribution of pillar diameter and height compared to the original template or metallic replica. This is likely because the HMDS (silicone oil) added to dilute the PDMS partially evaporated before the replicate fully cured, and further feature shrinkage due to low stiffness.

Following replication, we functionalized the replica with fluorinated silane (HTMS) after a brief 1 minute air plasma (PDC-001-HP, Harrick Plasma) activation of the surface. Hydrophobic functionalization increased both apparent advancing and receding contact angles to $\theta_{\mathrm{a}}^{\mathrm{app}} = 155 \pm 4°$ and $\theta_{\mathrm{r}}^{\mathrm{app}} = 148 \pm 8°$, exhibiting superhydrophobicity (see Supporting Information S.6).

An advantage of DT-NIL over other soft lithography methods for making high-aspect ratio (>3) nanoscale PDMS features is the ability to prevent feature collapse[32-34] by transferring a protective Au layer from the template to the replica. Our results showed that DT-NIL enables us to conformally coat the replica with a surface layer transferred from the template. In some cases, transferring material from the template may be undesirable when it covers the desired replica surface chemistry. However, it can be readily compensated by further functionalization if there is any specific material or function required of the replica.

The benefit of this Au layer transfer can be observed in SEMs of cicada wing replicas fabricated without the protective gold layer, clearly showing clusters of nanopillars stuck together or ‘kissing pillars’ (Figure S5a). We hypothesize that two explanations exist for

structural collapse: 1) collapse from capillary forces upon solvent drying, and 2) collapse from the low stiffness of the PDMS elastomer.[32] The former can be mitigated by drying the replicas with a low surface energy solvent such as supercritical CO_2.[34] Indeed, supercritical drying significantly reduces the collapse of nanopillars (Fig. S5b), however; it could not completely prevent collapse. This is due to the bending stresses present in high aspect ratio, low stiffness PDMS nanopillars. Therefore, to prevent these collapses, we sputter-coated a protective solid Au layer onto the nanopillars to enhance their structural stiffness (See Supporting Information S.7 for Au layer thickness and structural stiffness calculation.). After depositing a 5 nm gold layer onto the nanopillars they remain upright individually at the end of the entire fabrication process.

The DT-NIL technique is versatile for the replication of nanoscale features, as illustrated above by the variety of deposition techniques and materials used to replicate cicada wing nanopillars. The chemical and physical identity of the features to be copied, however, play a pivotal role in the achievable resolution. While the surface features of the cicada wing push the lower limit for size replication by our simple DT-NIL technique, we recognize that the nanopillars present on cicada wings are relatively simple in topography. Furthermore, the hydrophobic waxes and hydrocarbons[35] at the surface reduce surface adhesion, making them a good candidate for masters in the NIL process.[36] To further demonstrate the scalability and utility of DT-NIL for surfaces other cicada wings, we produced PDMS replicas of a hierarchical biological surface with re-entrant features as well as replicas of two rigid nanoengineered silicon surfaces.

The wings of the fly (*S. bullata*) possess hierarchical roughness and multiscale topographies of short nanopillars on the surface with microscale curved hairs extending from the wing (Fig. 4a). The microscale hairs extend up and curve back inward lateral to the surface,

forming a doubly re-entrant rod that is difficult to replicate using conventional NIL techniques. Using DT-NIL with PDMS as the material of choice, we were able to successfully replicate fly wings (Fig. 4b). The use of a fly wing master demonstrated the successful replication of surfaces with hierarchical structures with dimensions that scale over many orders of magnitude.[37, 38] In order to avoid nanoscale pillar or microscale hair collapse due to capillary drying during template removal, fly wing replication required the use of supercritical CO_2 drying. The replication of re-entrant structures from the master was possible because of the flexibility of both the fly hairs and the incompletely cured template resin before separation. If the resin is allowed to fully cure at this step in the process, the template becomes inflexible and is difficult to remove from the master, ripping off and damaging even flexible features such as the fly hairs. Once separated and fully cured, the resin template is hardened, but possesses all re-entrant features. Whether using a flexible replica material, such as PDMS, or an inflexible replica material, such as electrodeposited Cu, the replica and template are unlikely to separate without removing or damaging the re-entrant features if using a mechanical method of separation. Thus, the ability to dissolve away the template by chemical means is key and permits the use of a variety of replica materials.

The replication of small features present on flexible natural surfaces, which tend to have a low Young's modulus, using non-destructive DT-NIL shows the utility of the technique. To further demonstrate the approach on rigid substrates having ordered or random nanoscale features, we tested the method on two nanostructured silicon (Si) wafers having distinct structural morphologies. We first fabricated Si nanograss structures made from metal-assisted chemical etching using hydrofluoric acid (Figure 4c).[39] (For Si nanograss fabrication details, see Supporting Information S.8.) The Si nanograss was first silanized using HTMS through a

chemical vapor deposition method in order to ease the release of the template from the master by lowering the master's surface energy. The DT-NIL technique was able to replicate the Si nanograss features with PDMS, as shown in Figure 4d. The second Si nanostructure replicated was an array of nanopyramids with 600 nm base lengths and 800 nm pitch (Figure 4e).[40] The nanopyramids were fabricated using anisotropic wet etching of Si in a KOH solution, and electrodeposition of Ni. (For nanopyramid fabrication details, see Supporting Information S.8.) The SEM micrograph of the resulting PDMS replica, shown in Figure 4f, indicated the presence of distortion along the base of the pyramids. Interestingly, the use of the protective gold layer did not prevent distortion. Despite the distortion, AFM images and profiles of the nanopyramid template shows a full resolution negative structure (see Supporting Information S.9), indicating that DT-NIL produces an excellent template, and that distortion stems from shrink/swelling of the PDMS during replica formation.

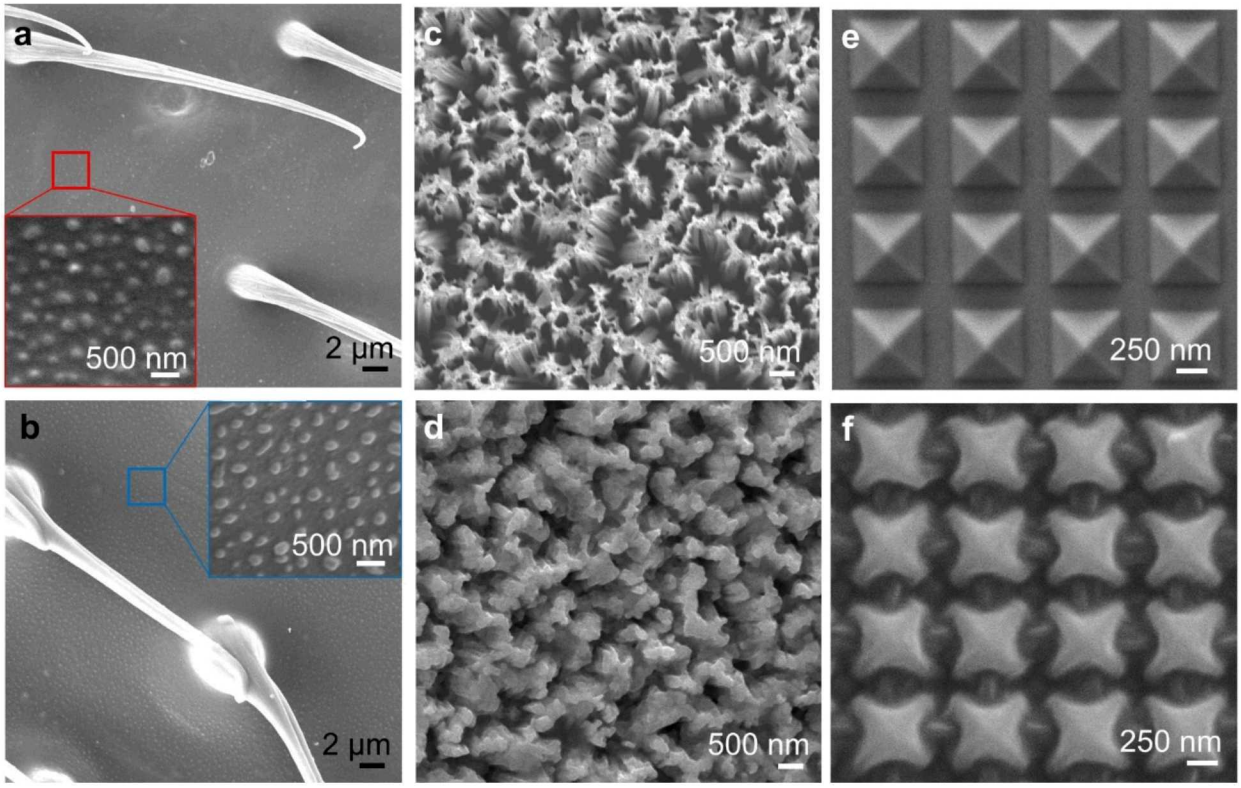

Figure 4. Biological and inorganic nanoengineered surfaces replicated using DT-NIL. (a) Original multiscale hierarchical and re-entrant features on fly wings (*S. bullata*) showing nanopillars beneath microscale hairs, and (b) replica of the fly wings fabricated using the DT-NIL method. The inset images in each figure show nanofeatures at the base underneath the hairs. (c) Si nanograss fabricated by metal-assisted chemical etching using HF and (d) replica of nanograss made with PDMS. (e) Array of nickel coated nanopyramids (L_{base} = 600 nm) made from KOH anisotropic etching of silicon substrates followed by nickel electrodepositon with corresponding (f) replica of the nanopyramids.

In this study, we develop a simple, scalable, cost-effective, and widely accessible nanoimprinting method using dissolvable templates made from commonly available nail polish and solvents. The DT-NIL method is capable of reproducing full resolution nanoscale replicas in both metal and elastomer materials. Although demonstrated here for Cu with electroplating, any alternative plating materials can be used. The DT-NIL method described here also has the potential to be developed further for the purpose of fabricating roll-to-roll (R2R-) or roll-to-plate (R2P-) NIL to increase scalability and throughput as the template is flexible and bendable.

The use of a dissolvable template imparts several key advantages over current NIL methods. First, DT-NIL can be performed at ambient conditions (pressure and temperature) without sophisticated equipment and using toxic materials such as photoresists. Second, the DT-NIL method can easily transfer metallic coatings onto replicas (when needed) that can help structurally stabilize elastomer nanostructures. Third, the DT-NIL method can replicate re-entrant, multiscale (micro or nanoscale), and hierarchical (micro and nanoscale) features having complex topographies. In the future, studies are needed on additional template solution chemistries with desired rheological properties that can enable optimal replication for specific applications beyond cicada wings. Fourth, DT-NIL is applicable to both hard and soft master materials for replication. Lastly, DT-NIL is particularly well suited for the replication of nanofeatures on surfaces that need to stay intact after replication (non-destructive). Even though the template cannot be reused, the replication process is so precise that it enables us to make one replica from a robust material (such as copper or silicon) and use that replica instead as additional master surfaces to scale up the replication process. We envision the DT-NIL technique as having potential for the *in-situ* or *in-vivo* study of rare insect and animal species with complex micro and nanofeatures as a nail polish is biocompatible and the replication can be done without the need to collect a large number of samples. In summary, the nanoimprinting method developed here demonstrates a facile, inexpensive, and highly versatile approach for achieving scalable nanofabrication of complex surface topographies for the replication of a range of natural and engineered surfaces.

ASSOCIATED CONTENT

Acknowledgments

This work was supported by the Army Basic Research Program through collaboration with the U.S. Army Engineer Research and Development Center, Construction Engineering Research Laboratory under grant number ARMY CESU W9132T-16-2-0011. J.O. and N.M. gratefully acknowledge funding support from the National Science Foundation under Award no. 1554249 and the International Institute for Carbon Neutral Energy Research (WPI-I2CNER), sponsored by the Japanese Ministry of Education, Culture, Sports, Science and Technology. Field-emission scanning electron microscopy and supercritical CO_2 drying was carried out at the Beckman Institute, University of Illinois at Urbana-Champaign (UIUC). Atomic force microscopy was carried out at the Materials Research Laboratory Central Facilities, UIUC. J.O. and N.M. also acknowledge Prof. Sheng Shen at Carnegie Mellon University for providing the nanopyramid surfaces for replica fabrication. The authors thank Todd Fulton (Dept. of Entomology, UIUC) for his fly rearing efforts.

Sandia National Laboratories is a multimission laboratory managed and operated by National Technology & Engineering Solutions of Sandia, LLC, a wholly-owned subsidiary of Honeywell International Inc., for the U.S. Department of Energy's National Nuclear Security Administration under contract DE-NA0003525. This paper describes objective technical results and analysis. Any subject views or opinions that might be expressed in the paper do not necessarily represent the views of the U.S. Department of Energy or the United States Government.

Supporting Information

Detailed discussion on reproducibility of the method, sample collection, nanopillar collapse and preventative measures, and viability of the method applicable to other types of surfaces.

References

1. Chou, S. Y.; Krauss, P. R.; Renstrom, P. J., Nanoimprint lithography. *Journal of Vacuum Science & Technology B: Microelectronics and Nanometer Structures Processing, Measurement, and Phenomena* **1996,** *14* (6), 4129-4133.
2. Guo, L. J., Nanoimprint Lithography: Methods and Material Requirements. *Advanced Materials* **2007,** *19* (4), 495-513.
3. Hong, S.-H.; Hwang, J.; Lee, H., Replication of cicada wing's nano-patterns by hot embossing and UV nanoimprinting. *Nanotechnology* **2009,** *20* (38), 385303.
4. Schift, H., Nanoimprint lithography: An old story in modern times? A review. *Journal of Vacuum Science & Technology B: Microelectronics and Nanometer Structures Processing, Measurement, and Phenomena* **2008,** *26* (2), 458-480.
5. Matsui, S.; Igaku, Y.; Ishigaki, H.; Fujita, J.; Ishida, M.; Ochiai, Y.; Komuro, M.; Hiroshima, H., Room temperature replication in spin on glass by nanoimprint technology. *Journal of Vacuum Science & Technology B: Microelectronics and Nanometer Structures Processing, Measurement, and Phenomena* **2001,** *19* (6), 2801-2805.
6. Khang, D. Y.; Yoon, H.; Lee, H. H., Room□Temperature Imprint Lithography. *Advanced Materials* **2001,** *13* (10), 749-752.
7. Otsuka, Y.; Hiwasa, S.; Taniguchi, J., Development of release agent-free replica mould material for ultraviolet nanoimprinting. *Microelectronic Engineering* **2014,** *123*, 192-196.
8. Cheng, X.; Guo, L. J.; Fu, P. F., Room-Temperature, Low-Pressure Nanoimprinting Based on Cationic Photopolymerization of Novel Epoxysilicone Monomers. *Advanced Materials* **2005,** *17* (11), 1419-1424.
9. Sreenivasan, S. V., Nanoimprint lithography steppers for volume fabrication of leading-edge semiconductor integrated circuits. *Microsystems & Nanoengineering* **2017,** *3* (1), 17075.
10. Ko, S. H.; Park, I.; Pan, H.; Grigoropoulos, C. P.; Pisano, A. P.; Luscombe, C. K.; Fréchet, J. M. J., Direct Nanoimprinting of Metal Nanoparticles for Nanoscale Electronics Fabrication. *Nano Letters* **2007,** *7* (7), 1869-1877.
11. Park, I.; Ko, S. H.; Pan, H.; Grigoropoulos, C. P.; Pisano, A. P.; Fréchet, J. M. J.; Lee, E. S.; Jeong, J. H., Nanoscale Patterning and Electronics on Flexible Substrate by Direct Nanoimprinting of Metallic Nanoparticles. *Advanced Materials* **2008,** *20* (3), 489-496.
12. Ryckman, J. D.; Liscidini, M.; Sipe, J. E.; Weiss, S. M., Direct Imprinting of Porous Substrates: A Rapid and Low-Cost Approach for Patterning Porous Nanomaterials. *Nano Letters* **2011,** *11* (5), 1857-1862.
13. Verschuuren, M. A.; Megens, M.; Ni, Y.; van Sprang, H.; Polman, A., Large area nanoimprint by substrate conformal imprint lithography (SCIL). *Advanced Optical Technologies* **2017,** *6* (3-4), 243-264.
14. Ahn, S. H.; Guo, L. J., Large-Area Roll-to-Roll and Roll-to-Plate Nanoimprint Lithography: A Step toward High-Throughput Application of Continuous Nanoimprinting. *ACS Nano* **2009,** *3* (8), 2304-2310.
15. Amsden, J. J.; Domachuk, P.; Gopinath, A.; White, R. D.; Negro, L. D.; Kaplan, D. L.; Omenetto, F. G., Rapid Nanoimprinting of Silk Fibroin Films for Biophotonic Applications. *Advanced Materials* **2010,** *22* (15), 1746-1749.
16. Ahn, S. H.; Guo, L. J., High-Speed Roll-to-Roll Nanoimprint Lithography on Flexible Plastic Substrates. *Advanced Materials* **2008,** *20* (11), 2044-2049.

17. Chang, T.-L.; Wang, J.-C.; Chen, C.-C.; Lee, Y.-W.; Chou, T.-H., A non-fluorine mold release agent for Ni stamp in nanoimprint process. *Microelectronic Engineering* **2008,** *85* (7), 1608-1612.
18. Kitagawa, T.; Nakamura, N.; Kawata, H.; Hirai, Y., A novel template-release method for low-defect nanoimprint lithography. *Microelectronic Engineering* **2014,** *123*, 65-72.
19. Traub, M. C.; Longsine, W.; Truskett, V. N., Advances in Nanoimprint Lithography. *Annual Review of Chemical and Biomolecular Engineering* **2016,** *7* (1), 583-604.
20. Oh, J.; Dana, C. E.; Hong, S.; Román, J. K.; Jo, K. D.; Hong, J. W.; Nguyen, J.; Cropek, D. M.; Alleyne, M.; Miljkovic, N., Exploring the Role of Habitat on the Wettability of Cicada Wings. *ACS Applied Materials & Interfaces* **2017,** *9* (32), 27173-27184.
21. Deegan, R. D.; Bakajin, O.; Dupont, T. F.; Huber, G.; Nagel, S. R.; Witten, T. A., Capillary flow as the cause of ring stains from dried liquid drops. *Nature* **1997,** *389* (6653), 827-829.
22. Popov, Y. O., Evaporative deposition patterns: Spatial dimensions of the deposit. *Physical Review E* **2005,** *71* (3), 036313.
23. Gu, Z.; Li, S.; Zhang, F.; Wang, S., Understanding Surface Adhesion in Nature: A Peeling Model. *Advanced Science* **2016,** *3* (7), 1500327.
24. Kelleher, S. M.; Habimana, O.; Lawler, J.; O'reilly, B.; Daniels, S.; Casey, E.; Cowley, A., Cicada wing surface topography: an investigation into the bactericidal properties of nanostructural features. *ACS applied materials & interfaces* **2015,** *8* (24), 14966-14974.
25. Murdan, S.; Bari, A.; Ahmed, S.; Hossin, B.; Kerai, L., Nail lacquer films' surface energies and in vitro water-resistance and adhesion do not predict their in vivo residence. *British Journal of Pharmacy* **2017,** *2* (1), 1-13.
26. Laba, D., *Rheological properties of cosmetics and toiletries*. Routledge: 2017.
27. Ji, S.; Park, J.; Lim, H., Improved antireflection properties of moth eye mimicking nanopillars on transparent glass: flat antireflection and color tuning. *Nanoscale* **2012,** *4* (15), 4603-4610.
28. Nam, Y.; Ju, Y. S., A comparative study of the morphology and wetting characteristics of micro/nanostructured Cu surfaces for phase change heat transfer applications. *Journal of Adhesion Science and Technology* **2013,** *27* (20), 2163-2176.
29. Odom, T. W.; Love, J. C.; Wolfe, D. B.; Paul, K. E.; Whitesides, G. M., Improved Pattern Transfer in Soft Lithography Using Composite Stamps. *Langmuir* **2002,** *18* (13), 5314-5320.
30. Watson, G. S.; Myhra, S.; Cribb, B. W.; Watson, J. A., Putative functions and functional efficiency of ordered cuticular nanoarrays on insect wings. *Biophysical Journal* **2008,** *94* (8), 3352-3360.
31. Morikawa, J.; Ryu, M.; Seniutinas, G.; Balčytis, A.; Maximova, K.; Wang, X.; Zamengo, M.; Ivanova, E. P.; Juodkazis, S., Nanostructured antireflective and thermoisolative cicada wings. *Langmuir* **2016,** *32* (18), 4698-4703.
32. Chandra, D.; Yang, S., Capillary-Force-Induced Clustering of Micropillar Arrays: Is It Caused by Isolated Capillary Bridges or by the Lateral Capillary Meniscus Interaction Force? *Langmuir* **2009,** *25* (18), 10430-10434.
33. Tawfick, S.; De Volder, M.; Hart, A. J., Structurally Programmed Capillary Folding of Carbon Nanotube Assemblies. *Langmuir* **2011,** *27* (10), 6389-6394.
34. Zhang, Y.; Lo, C.-W.; Taylor, J. A.; Yang, S., Replica Molding of High-Aspect-Ratio Polymeric Nanopillar Arrays with High Fidelity. *Langmuir* **2006,** *22* (20), 8595-8601.

35. Jessica Román-Kustas, J. B. H., Julian H. Reed, Andrew E. Gonsalves, Junho Oh, Longnan Li, Sungmin Hong, Kyoo D. Jo, Catherine E. Dana, Nenad Miljkovic, Donald M. Cropek, Marianne Alleyne, Molecular and Topographical Organization: Influence on Cicada Wing Wettability and Bactericidal Properties. *Advanced Materials Interfaces (Under Revision)* **2020**.
36. Zhang, G.; Zhang, J.; Xie, G.; Liu, Z.; Shao, H., Cicada Wings: A Stamp from Nature for Nanoimprint Lithography. *Small* **2006,** *2* (12), 1440-1443.
37. Yan, X.; Chen, F.; Sett, S.; Chavan, S.; Li, H.; Feng, L.; Li, L.; Zhao, F.; Zhao, C.; Huang, Z.; Miljkovic, N., Hierarchical Condensation. *ACS Nano* **2019,** *13* (7), 8169-8184.
38. Martin-Martinez, F. J.; Jin, K.; López Barreiro, D.; Buehler, M. J., The Rise of Hierarchical Nanostructured Materials from Renewable Sources: Learning from Nature. *ACS Nano* **2018,** *12* (8), 7425-7433.
39. Li, X.; Bohn, P. W., Metal-assisted chemical etching in HF/H2O2 produces porous silicon. *Applied Physics Letters* **2000,** *77* (16), 2572-2574.
40. Li, P.; Liu, B.; Ni, Y.; Liew, K. K.; Sze, J.; Chen, S.; Shen, S., Large-Scale Nanophotonic Solar Selective Absorbers for High-Efficiency Solar Thermal Energy Conversion. *Advanced Materials* **2015,** *27* (31), 4585-4591.

Graphic for Table of Contents